

Optimal phase synchronization in networks of phase-coherent chaotic oscillators

P. S. Skardal,^{1,a)} R. Sevilla-Escoboza,^{2,3} V. P. Vera-Ávila,^{2,3} and J. M. Buldú^{3,4}

¹Department of Mathematics, Trinity College, Hartford, Connecticut 06106, USA

²Centro Universitario de los Lagos, Universidad de Guadalajara, Enrique Díaz de León, Paseos de la Montaña, Lagos de Moreno, Jalisco 47460, Mexico

³Laboratory of Biological Networks, Center for Biomedical Technology, UPM, Pozuelo de Alarcón, 28223 Madrid, Spain

⁴Complex Systems Group & GISC, Universidad Rey Juan Carlos, 28933 Móstoles, Madrid, Spain

(Received 16 September 2016; accepted 2 January 2017; published online 12 January 2017)

We investigate the existence of an optimal interplay between the natural frequencies of a group of chaotic oscillators and the topological properties of the network they are embedded in. We identify the conditions for achieving phase synchronization in the most effective way, i.e., with the lowest possible coupling strength. Specifically, we show by means of numerical and experimental results that it is possible to define a synchrony alignment function $J(\omega, L)$ linking the natural frequencies ω_i of a set of non-identical phase-coherent chaotic oscillators with the topology of the Laplacian matrix L , the latter accounting for the specific organization of the network of interactions between oscillators. We use the classical Rössler system to show that the synchrony alignment function obtained for phase oscillators can be extended to phase-coherent chaotic systems. Finally, we carry out a series of experiments with nonlinear electronic circuits to show the robustness of the theoretical predictions despite the intrinsic noise and parameter mismatch of the electronic components. Published by AIP Publishing. [<http://dx.doi.org/10.1063/1.4974029>]

The emergence of synchronization of dynamical systems relies on three different aspects that are unavoidably connected: (i) the dynamical system under study, (ii) the kind of the coupling between dynamical units, and (iii) the structure of the network of connections. In this paper, we investigate how the distributions of the natural frequencies of a group of dynamical systems that are connected through a certain network topology are crucial to promote or hinder the emergence of phase-synchronization. We show that, given a specific network structure and a set of chaotic oscillators with a certain frequency distribution, there is an optimal allocation for each dynamical system according to its natural frequency. Thus, phase synchronization arises, or not, depending on the interplay between the dynamical and topological properties of the nodes. To verify the robustness of our theoretical predictions, we construct a network of nonlinear electronic circuits and check whether the predicted optimal allocation facilitates the arousal of phase-synchronization. Despite the fact that our results do not apply to non-phase-coherent chaotic oscillators, they demonstrate the existence of an interplay between the dynamical and topological properties of non-identical chaotic systems when trying to achieve strong synchronization.

has shown that the particular structure of connections between a system of nonlinear oscillators is crucial in determining the synchronization of the ensemble.³⁻⁵ Nevertheless, determining effective network structures for a given dynamical system is far from a trivial task. The many classes of dynamical systems, as well as the various types of synchronization we aim to achieve, result in the absence of a unique (or general) network structure maximizing the synchronizability of the system. To this end, it is necessary to understand, for each particular case, how the dynamical system and the structure of connections are intermingled. For example, in the case of heterogeneous phase oscillators such as the Kuramoto model,⁶ the degree heterogeneity of the network⁷ together with the spectral properties of the adjacency and Laplacian matrices⁴ can help us to identify what networks are more prone to synchronize and even to assess the time required to reach the synchronization manifold.⁸

When the state of the oscillators consists of more than just a single phase, possibly giving rise to chaotic dynamics, synchronization is more complicated. Nevertheless, for an ensemble of identical systems coupled with diffusive coupling, it is possible to obtain a Master Stability Function (MSF) indicating the ability of a system to synchronize by evaluating the stability of the synchronization manifold.⁹ Extensions of the MSF approach has been proposed for systems with slight parameter mismatch,¹⁰ but still require that the oscillators are *nearly* identical. More recently, it has been pointed out that not only the stability of the synchronized manifold, but the basin of attraction is crucial for the synchronization of the whole system, particularly in real-world scenarios and applications.¹¹ The identification of a basin of synchronization is especially useful in real systems where

I. INTRODUCTION

Synchronization of nonlinear dynamical systems have intrigued scientist in various disciplines studying the emergence of collective phenomena.^{1,2} A large body of research

^{a)}persebastian.skardal@trincoll.edu

the intrinsic parameter mismatch turns the MSF not applicable. Other approaches have been developed more recently, which allow a network to re-organize itself in the most adequate way. In this scenario, it has been demonstrated that the heterogeneity of the nodes can be a driving force behind the evolution of the network structure.^{12,13}

Within this framework, a recent work has identified a new perspective in the analysis of synchronization of heterogeneous systems. In Ref. 14, the authors show that given (i) a group of phase oscillators with heterogeneous natural frequencies and (ii) a given network structure, the precise location of the oscillators on the network has crucial consequences on the synchronization of the whole system. In particular, a *synchrony alignment function* (SAF) can be defined that describes the interplay between the natural frequencies and the networks structure, and serves as an objective measure of the synchronization of the network. Using the SAF, the synchronization properties of a network can be optimized by either (i) strategically allocating oscillators on a fixed network or (ii) tailoring a network to a fixed set of oscillators. This approach accounts for both the heterogeneity in the dynamics of the specific set of oscillators as well as the interactions dictated by the specific network structure. In other words, there is no unique optimal network structure universally valid for all possible sets of frequencies and networks—in general, they have different optimal configurations. Recent work has extended this approach to the case of directed networks,¹⁵ ranking network edges for synchronization¹⁶ and evaluating erosion of synchronization in networks.^{17,18}

In this paper, we translate the concepts introduced in Ref. 14 to the synchronization of chaotic oscillators. We hypothesize that phase-coherent chaotic oscillators with a clear dominant frequency can be treated as phase oscillators and, in turn, the SAF describing the optimal interplay between the natural frequencies and network topology could be used to optimize phase synchronization. Note that this heuristic argument relies on the fact that each dynamical unit is identified with a unique natural frequency, which is not the general case of chaotic oscillators. Nevertheless, this simplification is reasonable for phase coherent systems^{1,19,20} as long as their power spectrum of the dynamical system is narrow enough to clearly identify a dominant frequency. We demonstrate by means of numerical simulations and experiments with nonlinear electronic circuits that the SAF introduced in Ref. 14 is applicable to phase-coherent chaotic oscillators and can be used to find optimal configurations in networks of heterogeneous chaotic oscillators. We also show how the use of the SAF is robust both for random and scale-free topologies but can fail when non-phase-coherent chaotic systems are considered.

The remainder of this paper is organized as follows: In Sec. II, we describe the oscillator model we are considering and the optimization method using the SAF. In Sec. III, we present numerical results demonstrating the effectiveness of the optimization method for attaining phase synchronization in networks of chaotic oscillators. In Sec. IV, we validate these numerics by presenting experimental results using networks of nonlinear electronic circuits. In Sec. V, we conclude with a discussion of our results.

II. MODELS AND METHODS

We begin by describing the dynamical system under consideration. Specifically, we study networks of coupled Rössler oscillators,²¹ modified as in Ref. 22. We choose this class of oscillator due to the fact that they represent a paradigmatic example of a class of phase-coherent chaotic oscillators.¹ Next, we construct a network \mathcal{G} of N Rössler oscillators, which are diffusively coupled following the equations:

$$\dot{x}_i = -\alpha_i \left[\Gamma \left(x_i - d \sum_{j=1}^N a_{ij}(x_j - x_i) \right) + \beta y_i + \lambda z_i \right], \quad (1)$$

$$\dot{y}_i = -\alpha_i(-x_i + \nu y_i), \quad (2)$$

$$\dot{z}_i = -\alpha_i[-g(x_i) + z_i], \quad (3)$$

where

$$g(x) = \begin{cases} 0 & \text{if } x \leq 3 \\ \mu(x - 3), & \text{if } x > 3 \end{cases} \quad (4)$$

is the nonlinear function allowing the oscillators to have a chaotic output. The parameter d is the global coupling strength, each α_i determines the frequency of oscillator i , and the entries a_{ij} define the adjacency matrix $\mathbf{A}\{a_{ij}\}$ of network \mathcal{G} , such that $a_{ij} = 1$ if a link exists between oscillators i and j , and $a_{ij} = 0$ otherwise. Other parameters are $\Gamma = 0.05$, $\beta = 0.5$, $\lambda = 1$, $\mu = 15$, and $\nu = 0.2 - 10/R$, where $R = 100$. Under this parameter configuration, Rössler oscillators have a phase-coherent chaotic output in isolation (i.e., for $d = 0$), and their frequencies, ω_i , taken to be the position of the localized peak of the Fourier spectrum, are proportional to α_i . (This follows from the fact that, in isolation, the dynamics of oscillator i acts on a timescale of α_i^{-1}). The fact that oscillators are phase coherent allows us to evaluate their phase synchronization disregarding the behavior of their amplitude. In particular, we define the phase of oscillator i as the angle represented by the oscillator after projecting onto the xy -plane: $\theta_i = \arctan(y_i/x_i)$, as proposed in Ref. 23. Thus, the degree of phase synchronization of the network can be measured by the order parameter $r = |\sum_{j=1}^N e^{i\theta_j}|/N$. Here, we investigate how the particular frequency of each oscillator is related to the position it occupies in the network and how this relationship affects phase synchronization.

To explore the existence of an optimal frequency-structure interplay, we will adapt the methodological framework introduced in Refs. 14 and 15 to the case of phase-coherent chaotic oscillators. In these papers, the authors showed that the degree of phase synchronization in a network of heterogeneous phase oscillators is given by $r \approx 1 - J(\boldsymbol{\omega}, L)/2K^2$, where

$$J(\boldsymbol{\omega}, L) = \frac{1}{N} \sum_{j=2}^N \sigma_j^{-2} \langle \mathbf{u}^j, \boldsymbol{\omega} \rangle^2, \quad (5)$$

is the *synchrony alignment function* (SAF). Here, $\boldsymbol{\omega}$ is the vector of the natural frequencies of each oscillator and L is the network Laplacian whose entries are given by

$L_{ij} = \delta_{ij}k_i - A_{ij}$. In the case of symmetric adjacency and Laplacian matrices A and L , σ_j and \mathbf{w}^j are, respectively, the j th eigenvalue and associated eigenvector of L ,¹⁴ whereas in the case of asymmetric adjacency and Laplacian matrices A and L , σ_j and \mathbf{w}^j are, respectively, the j th singular value and associated left singular vector of L .¹⁵ We include a brief derivation of the SAF in Appendix A. Given the setup of the system in Eqs. (1)–(3), the heterogeneity of the parameters α_i makes both A and L asymmetric, and therefore, we use the asymmetric theory derived in Ref. 15. Given the relationship between r and $J(\omega, L)$, Eq. (5) can be used to maximize r (i.e., optimizing phase synchronization), in particular, by minimizing $J(\omega, L)$ via investigating different configurations of a given set of natural frequencies and/or networks.

III. NUMERICAL SIMULATIONS: LARGE NETWORKS OF PHASE COHERENT CHAOTIC OSCILLATORS

We begin by constructing networks of $N = 500$ nodes and $L = 1000$ links with an Erdős-Renyi random configuration.²⁴ Next, we introduce heterogeneity by assigning the pseudo-frequency parameters α_i randomly. Specifically, we obtain each α_i independently from a normal distribution with mean 10 and standard deviation 0.2. By doing so, complete synchronization of the whole network cannot be achieved, since systems are no longer identical. Instead, we aim to maximize the degree of phase synchronization using the SAF $J(\omega, L)$ whose input is the distribution of natural frequencies and the Laplacian matrices of the networks.

The alignment function is used in two different ways. We first consider *oscillator allocation*, where given a fixed network, we seek to arrange frequencies optimally on the network. To do so, we begin by allocating oscillators randomly and implement the following accept-reject algorithm: we propose a switch of two randomly chosen oscillators, and accept the switch only if the new arrangement yields a smaller value of $J(\omega, L)$, repeating this process for total number of proposed switches. In Figs. 1(a) and 1(b), we plot the results from simulations over a wide range of coupling strengths for networks with optimally allocated frequencies (blue circles), randomly allocated frequencies (red triangles), and poorly allocated frequencies (green crosses). Random allocations are given by the initial network and optimal allocations are obtained after 10^6 proposed switches. Poor allocations are similarly obtained, but aim to maximize $J(\omega)$ instead of minimizing it. Solid lines correspond to the average of $l = 50$ different random networks, and error bars indicate the standard deviation from the average. We note that optimally allocated set of oscillators performs remarkably well, as shown by the order parameter r (Fig. 1(a)), improving greatly on the random allocation with a sharp transition to a strongly synchronized state near $d \approx 0.2$. In addition, the synchronization error, obtained as $\epsilon = \frac{2}{N(N-1)} \sum_{i < j} |x_i - x_j|$ also captures the benefits of the optimal alignment (see Fig. 1(b)), despite the fact that it never vanishes (i.e., achieves perfect synchronization) due to the frequency mismatch of the oscillators. Moreover, phase synchronization can also be mitigated by maximizing $J(\omega, L)$ as demonstrated by the poorly allocated frequencies (green lines of Fig. 1).

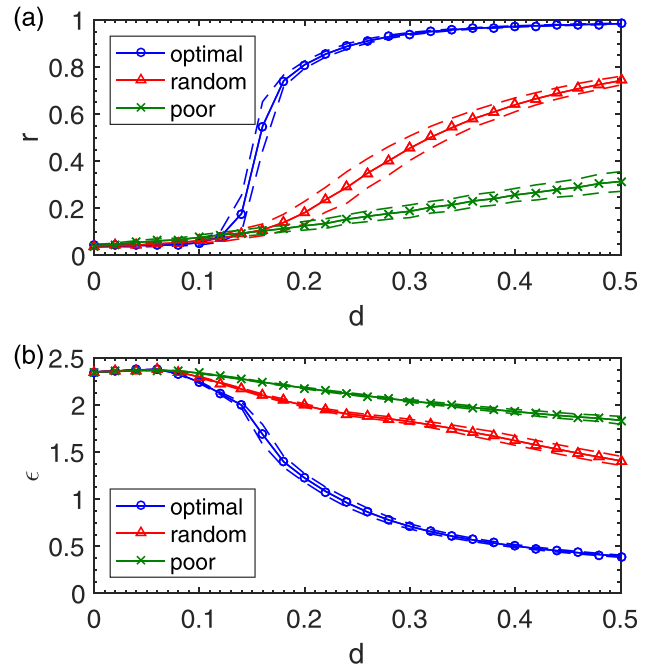


FIG. 1. Oscillator allocation. In (a), the order parameter r vs d (coupling strength) for optimal (blue circles), random (red triangles), and poor (green crosses) allocations of oscillators. Solid lines correspond to the average of the simulation of $l = 50$ Erdős-Renyi random networks of $N = 500$ nodes with $L = 1000$ links, while the error bars are their corresponding standard deviation. In (b), the corresponding synchronization error.

Second, we consider a *network design* approach, where given a set of oscillators with a predefined frequency distribution, we seek to build an optimal network structure promoting the phase synchronization of the whole ensemble. To do so, we initially allocate oscillators randomly on a network with a random configuration and implement a similar accept-reject algorithm: rather than switching two randomly chosen frequencies, we rewire a randomly chosen link. If the new network yields a smaller $J(\omega, L)$, we accept the rewiring, and otherwise we reject it. In Fig. 2(a), we plot the results of the order parameter r from simulations over a wide range of coupling strengths for optimal (blue circles), random (red triangles), and poor (green crosses) network structures. Random structures are given by the initial network, and optimal structures are obtained after 2×10^4 proposed rewirings. Poor structures are similarly obtained, but aim to maximize $J(\omega)$. As in the previous case, we note that the optimally rewired network performs much better than the random network, displaying a sharp transition to a strongly synchronized state similar to the case of oscillator allocation. The corresponding synchronization error ϵ also shows that complete synchronization never reached (Fig. 2(b)) due, again, to the heterogeneity of the frequency distribution. Again, phase synchronization can be mitigated by finding poor network structures.

Finally, we explore how the SAF methodology performs in two other cases. In Fig. 3(a), we show the order parameter of oscillator allocation when the underlying network has scale-free structure. Specifically, we consider networks with $N = 500$ nodes with scale-free degree distributions $P(k) \propto k^{-\gamma}$ for $\gamma = 3$ and minimum degree $k_0 = 2$, obtained with the configuration model.²⁵ Similar qualitative results are

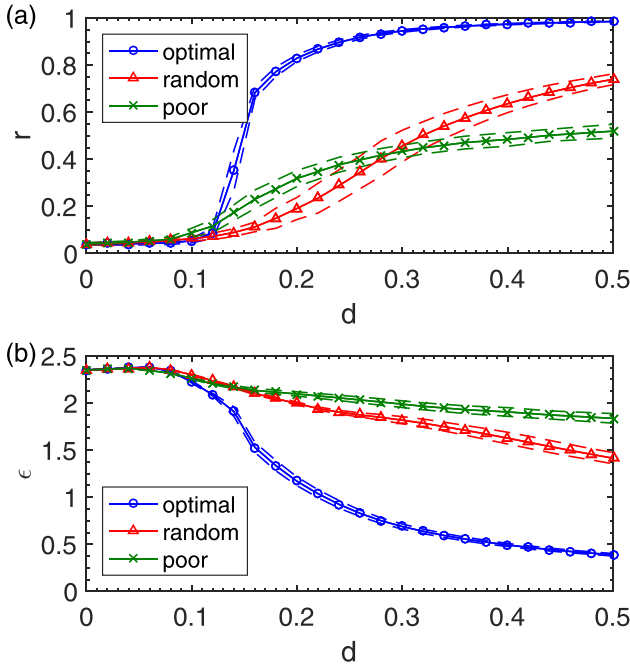


FIG. 2. Network design. In (a), the order parameter r vs d (coupling strength) for optimal (blue circles), random (red triangles), and poor (green crosses) network structures. Solid lines correspond to the average of the simulation of $l=50$ Erdős-Renyi random networks of $N=500$ nodes with $L=1000$ links, while the error bars are their corresponding standard deviation. In (b), the corresponding synchronization error.

obtained both for the oscillator allocation and the network reconfiguration (the latter not shown here). In Fig. 3(b), the dynamical system has been replaced by a Lorenz system,^{26,27} which is a paradigmatic example of a chaotic system that it is not phase-coherent. We summarize the dynamics and phase description of the Lorenz system in Appendix B. In this case, the ambiguity in the phase definition leads to a difficulty in defining a characteristic frequency for each oscillator, which in turn hinders the SAF methodology in obtaining optimal configurations of frequencies and network topologies. In particular, we see that networks with “optimally” allocated frequencies (blue circles) perform no better than randomly allocated (red triangles) or “poorly” allocated (green crosses) frequencies in terms of phase synchronization or the synchronization error (inset).

IV. EXPERIMENTAL RESULTS: IMPLEMENTATION WITH NONLINEAR ELECTRONIC CIRCUITS

Next, we validate the robustness of the previous results with a real experiment based on an electronic implementation of a network of Rössler oscillators. The experimental design of the whole network, and its control, is shown in Figure 4. It consists of an electronic array (EA), a multifunction data card (DAQ), and a personal computer (PC). The EA comprises 20 Rössler-like electronic circuits (see Ref. 28 for a detailed description of the electronic schemes) forming a network, whose structure can be modified maintaining the degree of each node. Thus, as a contrast to the numerical results above, the EA is small in size. We translate variables x_i , y_i , and z_i and all the parameters appearing in Eqs. (1)–(3)

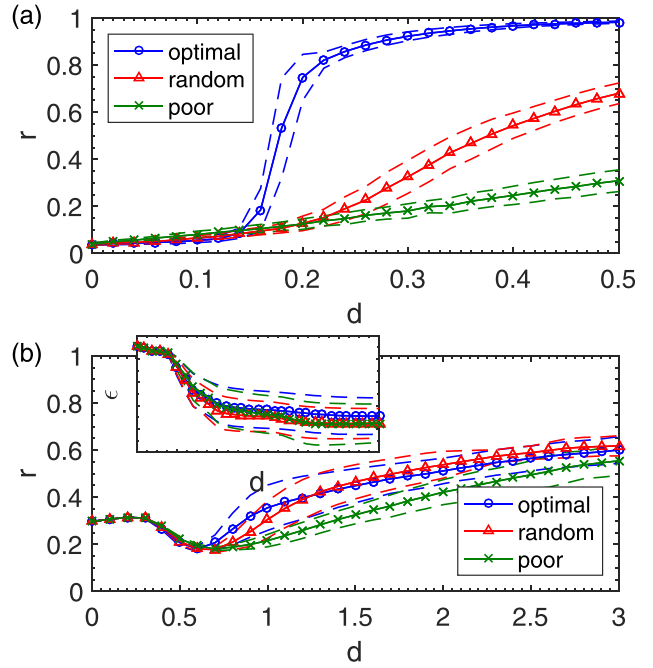


FIG. 3. Performance of the alignment function in other cases. In (a), the order parameter r vs d (coupling strength) for optimal (blue circles), random (red triangles), and poor (green crosses) allocations of oscillators on scale-free networks. Solid lines correspond to the average of the simulation of $l=50$ networks with scale-free degree distribution $P(k) \propto k^{-\gamma}$ for $\gamma=3$ and minimum degree $k_0=2$. Error bars indicate standard deviation. In (b), the order parameter r vs d (coupling strength) for optimal (blue circles), random (red triangles), and poor (green crosses) allocations of Lorenz oscillators. Inset: the corresponding synchronization error. Solid lines correspond to the average of the simulation of $l=50$ Erdős-Renyi random networks of $N=500$ nodes with $L=1000$ links, while the error bars are their corresponding standard deviation.

to the three voltages v_{1i} , v_{2i} , and v_{3i} and a combination of different electronic components, leading to the following circuit equations:

$$v_{1i}(t) = -\frac{1}{R_1 C_1} \left(v_{1i} + \frac{R_1}{R_2} v_{2i} + \frac{R_1}{R_4} v_{3i} - d \frac{R_1}{R_{15}} \sum_{j=1}^N A_{ij} [v_{1j} - v_{1i}] \right), \tag{6}$$

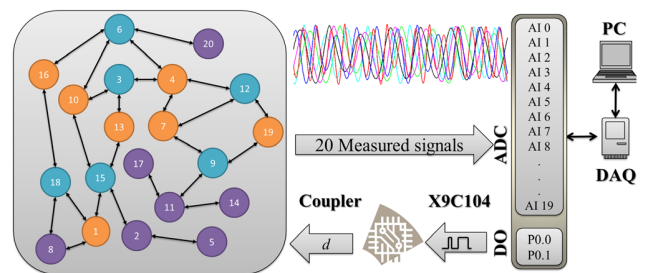


FIG. 4. Experimental setup. On the left, schematic representation of the coupling topology of the 20-circuit network, which can be modified according to the predictions given by the alignment function. The total number of links is always maintained to $L=25$. The coupling strength d is adjusted by means of one digital potentiometers X9C104 controlled by a signal coming from the digital ports P0.0–P0.1 of a DAQ Card. The outputs of the circuit are sent to a set of voltage followers that act as buffers and, then, sent to the analog ports (AI 0; AI 1; ...; AI 19) of the same DAQ Card. The whole experiment is controlled from a PC with Labview 8.5.

$$v_{2i}(t) = -\frac{1}{R_6 C_2} \left(-\frac{R_6 R_8}{R_9 R_7} v_{1i} + \left[1 - \frac{R_6 R_8}{R_c R_7} \right] v_{2i} \right), \quad (7)$$

$$v_{3i}(t) = -\frac{1}{R_{10} C_3} \left(-\frac{R_{10}}{R_{11}} G_{v_{1i}} + v_{3i} \right), \quad (8)$$

where

$$G_{x_i} = \begin{cases} 0 & \text{if } x \leq Id + Id \frac{R_{14}}{R_{13}} + Vee \frac{R_{14}}{R_{13}} \\ \frac{R_{12}}{R_{14}} x_i - Vee \frac{R_{12}}{R_{13}} - Id \left(\frac{R_{12}}{R_{13}} + \frac{R_{12}}{R_{14}} \right) & \text{if } x > Id + Id \frac{R_{14}}{R_{13}} + Vee \frac{R_{14}}{R_{13}}. \end{cases} \quad (9)$$

The values of all electronic components are summarized in Table I. Importantly, all chaotic oscillators have the same internal parameters with the exception of the capacitances C_i that, in turn, define the natural frequency of oscillation of each unit. This way, capacitances take different values for the set $C_i = \{2.2 \text{ nF}, 3.3 \text{ nF}, 4.7 \text{ nF}\}$, leading to a distribution of frequencies within the interval (240 – 540) Hz. The relation between α_i of the theoretical model and the capacitances is given by $\alpha_{v_{1i}} = \frac{1}{R_i C_i}$, $\alpha_{v_{2i}} = \frac{R_8}{R_7 R_9 C_2}$, and $\alpha_{v_{3i}} = \frac{1}{C_3 R_{10}}$. As a consequence, we obtain an ensemble of oscillators whose natural frequencies ω_i , in isolation, are inversely proportional to the value of the capacitances. Note that, due to the tolerance of the electronic components (between 5% and 10%), the frequencies of the oscillators also suffer a dispersion that goes beyond the nominal values of the capacitances. Figure 5 shows the power spectrum of the $N=20$ oscillators for $d=0$, i.e., in isolation. Each Rössler circuit has an individual electronic coupler controlled by a digital potentiometer (XDCP), which is adjusted by a digital signal coming from ports P0.0–1 (see Fig. 4). The digital port P0.0 is used to set the value of the coupling resistance (d), while port P0.1 increases/decreases the resistance of a voltage divisor controlling the final coupling strength d (and allowing to test 100 discretized values of d). All the experimental process is controlled by a virtual interface developed in Labview, which can be considered as a state machine. This way, the experimental procedure is as follows: first, d is set to zero, after a waiting time of 500 ms (roughly corresponding to $P = (120 - 270)$ cycles of the autonomous systems), the signals corresponding to the $x(t)$ variables of the 20 circuits are acquired by the analog ports (AI 0; AI 1; ...; AI 19).

TABLE I. Values of the electronic components used for the construction of the electronic version of the Rössler system.

C_{1-3}	2.2 nF	3.3 nF	4.7 nF
$R_1 = 2 \text{ M}\Omega$	$R_2 = 200 \text{ k}\Omega$	$R_3 = 10 \text{ k}\Omega$	$R_4 = 100 \text{ k}\Omega$
$R_5 = 50 \text{ k}\Omega$	$R_6 = 5 \text{ M}\Omega$	$R_7 = 100 \text{ k}\Omega$	$R_8 = 10 \text{ k}\Omega$
$R_9 = 10 \text{ k}\Omega$	$R_{10} = 100 \text{ k}\Omega$	$R_{11} = 100 \text{ k}\Omega$	$R_{12} = 150 \text{ k}\Omega$
$R_{13} = 68 \text{ k}\Omega$	$R_{14} = 10 \text{ k}\Omega$	$R_{15} = 100 \text{ k}\Omega$	$R_c = R_3 + R_5$
$Id = 0.7$	$Vee = 15$	$d = [0 - 0.6]$	

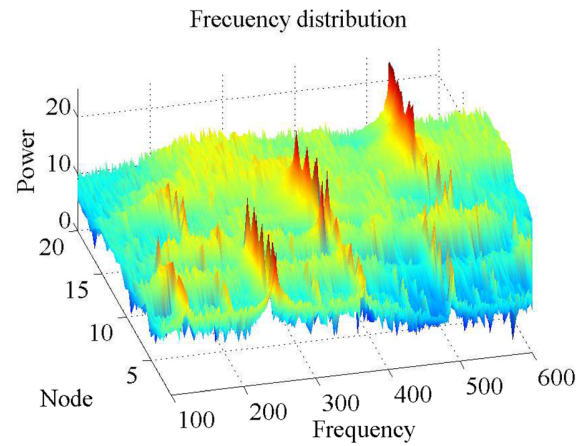


FIG. 5. Frequency distribution of the electronic Rösslers. Internal capacitances control the frequency of the $N=20$ Rössler circuits, taking a value from the set $C_i = \{2.2 \text{ nF}, 3.3 \text{ nF}, 4.7 \text{ nF}\}$. The “natural frequency” of each oscillator is obtained from the position of the maximum of their corresponding power spectrum.

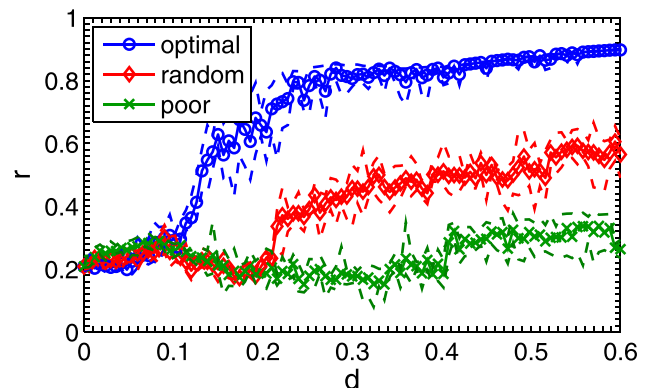


FIG. 6. Experimental test of the optimal alignment. Order parameter r of a network of heterogeneous Rössler circuits as a function of the coupling strength d and for a given network structure (see Fig. 4 for a representation of the network). Three different allocations are shown: the optimal alignment predicted by Eq. (5) (blue circles), a random configuration (red diamonds), and a poor allocation (green crosses). Dashed lines are the corresponding standard deviations obtained from five different experimental realizations.

Once this is recorded, the value of d is increased by one step, and the process is repeated until the maximum value of d is reached.

Once the $x_i(t)$ variable of all circuits is recorded, we obtain the equivalent instantaneous phase as $\phi_i(t) = 2\pi l_i + 2\pi \frac{t-t_i}{t_{i+1}-t_i}$, for each interval $t_i \leq t < t_{i+1}$, where t_i and t_{i+1} are the times of consecutive maxima of the variable $x_i(t)$.¹ It is important to remark that, for phase coherent systems, such a measure of instantaneous phase is fully equivalent to the geometrical phases used in the numerical simulations.⁴

Next, we evaluate the performance of the theoretical predictions given by the alignment function $J(\omega, L)$. We

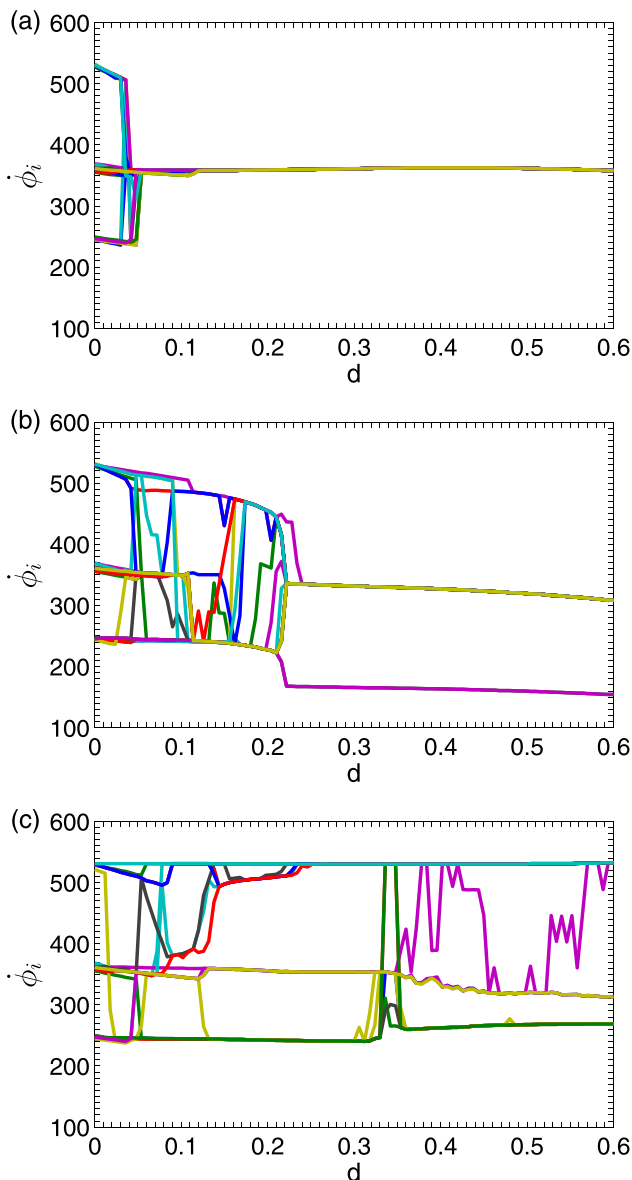


FIG. 7. Instantaneous frequency vs coupling strength d for different network alignments. In all figures, we plot the position of the highest peak of the power spectrum of each oscillator as a function of d . In (a), the optimal alignment leads to a frequency locking for couplings strengths higher than $d \sim 0.5$. In (b), a random allocation of the oscillators leads to the formation of synchronization clusters even for high values of the coupling strength. Finally, in (c), the poor allocation results in the coexistence of synchronization clusters together with a frequency drift of certain oscillators.

construct the specific network structure shown in Fig. 4, i.e., $N=20$ Rössler oscillators with the frequency distribution shown in Fig. 5 and with a fixed average degree of $\langle k \rangle = 2.5$. Next, we obtain the synchronization parameter r vs the coupling strength for three different configurations: (i) the optimal allocation according to an alignment function whose input are the average frequency of the oscillators and the Laplacian matrix of the network; (ii) a random allocation of the oscillators on the network, and finally, (iii) a poor allocation (i.e., maximizing the alignment function). Figure 6 shows how the optimal allocation allows the ensemble of oscillators to synchronize at lower coupling strengths and at the same time to reach higher values of the order parameter. A further inspection of the oscillators' instantaneous frequency reveals the path to synchronization for both the optimal and random allocations. Figure 7 shows the instantaneous frequency of the N oscillators, indicated by the position of the highest peak of their corresponding power spectrum, as the coupling strength d is increased. When the optimal alignment is implemented (Fig. 7(a)), we observe a frequency locking occurring at $d \sim 0.5$, which precedes the subsequent phase locking of the whole system reached for values of $d > 0.1$ (see blue line in Fig. 6). Interestingly, Figs. 7(b) and 7(c) show that deviations from the optimal alignment lead to, respectively, (b) the formation of frequency locked clusters preventing the whole system to synchronize and (c) the drift of a series of oscillators along the dominant frequencies of the system. In this way, we can observe that, in the case of random allocation, we obtain two different clusters of synchronization, which hold even for large values of d and prevent to achieve the phase synchronization of the whole system (Fig. 6(b)). In the case of the network with the poor allocation, the situation is even worse, since a series of oscillators drift from cluster to cluster leading to an even lower value of the order parameter. It is worth mentioning that, in Ref. 14, a positive correlation between ω_i and k_i was reported. However, such correlations are not observed in our experiments, which can be attributed to the finite size effects related to the experimental limitations resulting in a low heterogeneity in the number of nodes ($N=20$), natural frequencies (only three different frequencies are implemented), and node degrees ($1 \leq k \leq 4$).

V. CONCLUSIONS

Our results show, both numerically and experimentally, that when aiming to synchronize a network of phase-coherent chaotic systems, there exists an optimal alignment between the frequency of the oscillators and the topological properties of the network. The existence of an optimal correlation is shown from two perspectives: (i) promoting synchronization by the correct allocation of a group of heterogeneous oscillators over a given network structure and (ii) allowing the network to reorganize according to an alignment function. In both cases, the alignment function introduced in Ref. 14 for Kuramoto oscillators correctly defines the optimal frequency-topology correlation for Rössler systems with phase-coherent chaotic behavior.

At the same time, our results raise a series of questions to be addressed in the future. First, we have seen that the

application of the alignment function to the Lorenz system does not give successful results. This fact suggests that the alignment function of chaotic oscillators that are not phase-coherent needs to include, somehow, the complexity of the dynamics and not only the dominant frequency of the system. More generally, it raises the question of how to define new alignment functions accounting for power spectra with large dispersion. Is it possible to define a specific alignment function to each considered dynamical system? What is the relation between the optimal topologies for different dynamical systems? Both questions require significant attention in the near future and might be addressed in part by the SAF approach used here with of other approaches.^{29,30} In addition, it would be interesting to carry out experiments with a number of nodes two or three orders of magnitude higher, which would allow to check the theoretical predictions regarding the generality of our results in scale-free networks (which require a high number of nodes) and the expected correlations between the degree of the nodes and their natural frequencies.

On the other hand, there is a pristine field concerned about the identification of optimal topologies in real systems. For example, in brain networks, recent works have focused on the interplay between the dynamical and topological properties of different brain regions, and how the underlying physical connections constrain the functional networks associated with different cognitive and motor tasks.^{31–34} In this respect, the identification of alignment functions could help to understand the interplay between structural and functional networks. How close the actual configuration of a functional network is from the optimal topology and how a neurodegenerative disease may alter the possible alignment between dynamical and structural properties would be promising applications.

ACKNOWLEDGMENTS

The authors acknowledge D. Papo, R. Gutiérrez, and P. L. del Barrio for fruitful conversations. J.M.B. is funded by MINECO (FIS2013-41057-P). R.S.E. acknowledges Universidad de Guadalajara, Culagos (Mexico), for financial support (PIFI 522943 (2012), Becas Movilidad 290674-CVU-386032), and Secretaria de Educación Pública, PRODEP, UDG-PTC-1289-DSA/103.5/16/10313. P.S.S. acknowledges financial support from the James S. McDonnell Foundation.

APPENDIX A: DERIVATION OF THE SYNCHRONY ALIGNMENT FUNCTION

In this Appendix, we present a short derivation of the synchrony alignment function (SAF) as first described in Ref. 14. We consider a network of N phase oscillators evolving according to

$$\dot{\theta}_i = \omega_i + d \sum_{j=1}^N a_{ij} H(\theta_j - \theta_i), \quad (\text{A1})$$

where H is a coupling function which we assume satisfies $H'(0) > 0$ and $|H(0)/\sqrt{2}H'(0)| \ll 1$ to ensure the possibility of synchronization (this last condition ensures that the

coupling *frustration* is sufficiently small¹⁷). We then consider the *strong coupling regime* where a strongly synchronized state, i.e., $r \approx 1$, can be attained such that the difference between any two network-adjacent phases is small, $|\theta_j - \theta_i| \ll 1$. In this scenario, Eq. (A1) can be linearized to

$$\dot{\theta}_i \approx \tilde{\omega}_i - \tilde{d} \sum_{j=1}^N L_{ij} \theta_j, \quad (\text{A2})$$

where $\tilde{\omega}_i = \omega_i + KH(0)k_i$ and $\tilde{d} = dH'(0)$. Note that in the case of Kuramoto coupling where $H(\theta) = \sin \theta$, we have that $\tilde{\omega}_i = \omega_i$ and $\tilde{d} = d$. Dropping the \sim -notation, we next enter the rotating frame $\theta \rightarrow \theta + \Omega t$ where Ω is the collective frequency variation.³⁵ The stationary solution of Eq. (A2) can then be written in vector form

$$\theta^* = L^\dagger \omega / d, \quad (\text{A3})$$

where L^\dagger is the Moore-Penrose pseudoinverse of the Laplacian L .³⁶ In particular, if L is symmetric its pseudoinverse is defined by its eigen decomposition, $L^\dagger = \sum_{j=2}^N \sigma_j^{-1} \mathbf{u}^j \mathbf{u}^{jT}$, where σ_j and \mathbf{u}^j are, respectively, the j th eigenvalue and associated eigenvector of L . However, if L is asymmetric, its pseudoinverse is defined by its singular value decomposition, $L^\dagger = \sum_{j=2}^N \sigma_j^{-1} \mathbf{u}^j \mathbf{v}^{jT}$, where σ_j , \mathbf{u}^j , and \mathbf{v}^j are, respectively, the j th singular value, associated left singular vector, and associated right singular vectors of L . Finally, noting that to leading order the order parameter can be written

$$r \approx 1 - \frac{\|\theta^*\|^2}{2N}, \quad (\text{A4})$$

we insert Eq. (A3) into Eq. (A4) to obtain

$$r \approx 1 - J(\omega, L) / 2K^2, \quad (\text{A5})$$

where

$$J(\omega, L) = \frac{1}{N} \sum_{j=2}^N \sigma_j^{-2} \langle \mathbf{u}^j, \omega \rangle^2 \quad (\text{A6})$$

is the SAF presented in the main text in Eq. (5).

APPENDIX B: DESCRIPTION OF THE LORENZ DYNAMICS

Here, we briefly describe the dynamics and phase description of the Lorenz oscillators used in the main text. Given a network of N nodes, we consider the following system:

$$\dot{x}_i = \alpha_i [\sigma(x_i - y_i) + d \sum_{j=1}^N a_{ij} (x_j - x_i)], \quad (\text{B1})$$

$$\dot{y}_i = \alpha_i [x_i(\rho - z_i) - y_i], \quad (\text{B2})$$

$$\dot{z}_i = \alpha_i [x_i y_i - \beta z_i]. \quad (\text{B3})$$

As in the case of the Rössler oscillators, d represents a global coupling parameter, the entries a_{ij} describe the network structure, and α_i^{-1} determines the timescale of oscillator i . Other parameters are chosen $\sigma = 10$, $\rho = 28$, and $\beta = 8/3$ to

induce a chaotic state. The topology of the chaotic Lorenz attractor, however, is not phase-coherent making a phase θ_i difficult to be extracted from the state $(x_i, y_i, z_i)^T$. Here, we define a phase, first by defining the variable $u_i = \sqrt{x_i^2 + y_i^2}$, then defining θ_i as the angle made by the state (u_i, z_i) around the unstable fixed point $(u^*, z^*) = (\sqrt{2\beta(\rho - 1)}, \rho - 1)$, i.e.,

$$\theta_i = \arctan(z_i - (\rho - 1), u_i - \sqrt{2\beta(\rho - 1)}). \quad (\text{B4})$$

Using this formalism of each phase θ_i , the degree of phase synchronization is then given by the same order parameter as defined in the main text.

- ¹A. Pikovsky, M. Roseblum, and J. Kurths, *Synchronization: A Universal Concept in Nonlinear Sciences* (Cambridge University Press, Cambridge, UK, 2001).
- ²S. Boccaletti, J. Kurths, G. Osipov, D. L. Valladares, and C. S. Zhou, "The synchronization of chaotic systems," *Phys. Rep.* **366**, 1–101 (2002).
- ³S. Boccaletti, V. Latora, Y. Moreno, M. Chavez, and D. U. Hwang, *Phys. Rep.* **424**, 175–308 (2006).
- ⁴A. Arenas, A. Díaz-Guilera, J. Kurths, Y. Moreno, and C. Zhou, "Synchronization in complex networks," *Phys. Rep.* **469**, 93–153 (2008).
- ⁵M. E. J. Newman, *Networks: An Introduction* (Oxford University Press, New York, 2010).
- ⁶J. A. Acebrón, L. L. Bonilla, C. J. Pérez-Vicente, F. Ritort, and R. Spigler, "The Kuramoto model: A simple paradigm for synchronization phenomena," *Rev. Mod. Phys.* **77**, 137–185 (2005).
- ⁷J. G. Restrepo, E. Ott, and B. R. Hunt, "Onset of synchronization in large networks of coupled oscillators," *Phys. Rev. E* **71**, 036151 (2005).
- ⁸J. A. Almendral and A. Díaz-Guilera, "Dynamical and spectral properties of complex networks," *New J. Phys.* **9**, 187 (2007).
- ⁹L. M. Pecora and T. L. Carroll, "Master stability functions for synchronized coupled systems," *Phys. Rev. Lett.* **80**, 2109 (1998).
- ¹⁰J. Sun, E. M. Bollt, and T. Nishikawa, "Master stability functions for coupled nearly identical dynamical systems," *Europhys. Lett.* **85**, 60011 (2009).
- ¹¹P. J. Menck, J. Heitzig, N. Marwan, and J. Kurths, "How basin stability complements the linear-stability paradigm," *Nat. Phys.* **9**, 89–92 (2013).
- ¹²D. Kelly and G. A. Gottwald, "On the topology of synchrony optimized networks of a Kuramoto-model with non-identical oscillators," *Chaos* **21**, 025110 (2011).
- ¹³F. Scafuti, T. Aoki, and M. di Bernardo, "Heterogeneity induces emergent functional networks for synchronization," *Phys. Rev. E* **91**, 062913 (2015).
- ¹⁴P. S. Skardal, D. Taylor, and J. Sun, "Optimal synchronization of complex networks," *Phys. Rev. Lett.* **113**, 144101 (2014).
- ¹⁵P. S. Skardal, D. Taylor, and J. Sun, "Optimal synchronization of directed complex networks," *Chaos* **26**, 094807 (2016).
- ¹⁶D. Taylor, P. S. Skardal, and J. Sun, "Synchronization of heterogeneous oscillators under network modifications: Perturbations and optimization of the synchrony alignment function," *SIAM J. Appl. Math.* **76**, 1984 (2016).
- ¹⁷P. S. Skardal, D. Taylor, J. Sun, and A. Arenas, "Erosion of synchronization in networks of coupled oscillators," *Phys. Rev. E* **91**, 01802(R) (2015).
- ¹⁸P. S. Skardal, D. Taylor, J. Sun, and A. Arenas, "Erosion of synchronization: Coupling heterogeneity and network structure," *Physica D* **323–324**, 40 (2016).
- ¹⁹D. Farmer, J. Crutchfield, H. Froehling, N. Packard, and R. Shaw, "Power spectra and mixing properties of strange attractors," *Ann. N.Y. Acad. Sci.* **357**, 453 (1980).
- ²⁰M. G. Rosenblum, A. S. Pikovsky, and J. Kurths, "Phase synchronization of chaotic oscillators," *Phys. Rev. Lett.* **76**, 1804 (1996).
- ²¹O. E. Röessler, "An equation for continuous chaos," *Phys. Lett. A* **57**, 397 (1976).
- ²²I. Leyva, R. Sevilla-Escoboza, J. M. Buldú, I. Sendiña-Nadal, J. Gomez-Gardeñes, A. Arenas, Y. Moreno, S. Gomez, R. Jaimes-Reátegui, and S. Boccaletti, "Explosive first-order transition to synchrony in networked chaotic oscillators," *Phys. Rev. Lett.* **108**, 168702 (2012).
- ²³A. S. Pikovsky, M. G. Rosenblum, and J. Kurths, "Synchronization in a population of globally coupled chaotic oscillators," *Europhys. Lett.* **34**, 165–170 (1996).
- ²⁴P. Erdős and A. Rényi, "On random graphs. I," *Publ. Math.* **6**, 290–297 (1959).
- ²⁵A. Bekessy, P. Bekessy, and J. Komlos, "Asymptotic enumeration of regular matrices," *Stud. Sci. Math. Hung.* **7**, 343 (1972).
- ²⁶E. N. Lorenz, "Deterministic nonperiodic flow," *J. Atmos. Sci.* **20**, 130–141 (1963).
- ²⁷L. Huang, Q. Chen, Y.-C. Lai, and L. M. Pecora, "Generic behavior of master-stability functions in coupled nonlinear dynamical systems," *Phys. Rev. E* **80**, 036204 (2009).
- ²⁸R. Sevilla-Escoboza and J. M. Buldú, "Synchronization of networks of chaotic oscillators: Structural and dynamical datasets," *Data Brief* **7**, 1185–1189 (2016).
- ²⁹G. Gottwald, "Model reduction for networks of coupled oscillators," *Chaos* **25**, 053111 (2015).
- ³⁰R. S. Pinto and A. Saa, "Optimal synchronization of Kuramoto oscillators: A dimensional reduction approach," *Phys. Rev. E* **92**, 062801 (2015).
- ³¹T. Simas, M. Chavez, P. R. Rodríguez, and A. Díaz-Guilera, "An algebraic topological method for multimodal brain networks comparisons," *Front. Psychol.* **6**, 904 (2015).
- ³²C. J. Stam, E. C. van Straaten, E. Van Dellen, P. Tewarie, G. Gong, A. Hillebrand, J. Meier, and P. Van Mieghem, "The relation between structural and functional connectivity patterns in complex brain networks," *Int. J. Psychophysiol.* **103**, 149–160 (2016).
- ³³P. Garcés, E. Pereda, J. A. Hernández-Tamames, F. Del-Pozo, F. Maestú, and J. Pineda-Pardo, "Multimodal description of whole brain connectivity: A comparison of resting state MEG, fMRI, and DWI," *Human Brain Mapp.* **37**, 20–34 (2016).
- ³⁴F. Battiston, V. Nicosia, M. Chavez, and V. Latora, see <https://arxiv.org/abs/1606.09115> for "multilayer motif analysis of brain networks."
- ³⁵P. S. Skardal, D. Taylor, J. Sun, and A. Arenas, "Collective frequency variation in network synchronization and reverse PageRank," *Phys. Rev. E* **93**, 042314 (2016).
- ³⁶A. Ben-Israel and T. N. E. Grenville, *Generalized Inverses* (Springer, New York, 1974).